Crystallographic and Solution Studies of *N*-Lithocholyl Insulin: A New Generation of Prolonged-Acting Human Insulins†

Jean L. Whittingham,‡ Ib Jonassen,§ Svend Havelund,§ Shirley M. Roberts,‡ Eleanor J. Dodson,‡ Chandra S. Verma,‡,|| Anthony J. Wilkinson,‡ and G. Guy Dodson*,‡

Structural Biology Laboratory, Department of Chemistry, University of York, York YO10 5YW, U.K., Novo Nordisk A/S, Novo Allé, 2880 Bagsvaerd, Denmark, and Bioinformatics Institute, 30 Biopolis Way, 07-01 Matrix, Singapore 138671

Received December 2, 2003; Revised Manuscript Received March 10, 2004

ABSTRACT: The addition of specific bulky hydrophobic groups to the insulin molecule provides it with affinity for circulating serum albumin and enables it to form soluble macromolecular complexes at the site of subcutaneous injection, thereby securing slow absorption of the insulin analogue into the blood stream and prolonging its half-life once there. *N*-Lithocholic acid acylated insulin [Lys^{B29}-lithocholyl des-(B30) human insulin] has been crystallized and the structure determined by X-ray crystallography at 1.6 Å resolution to explore the molecular basis of its assembly. The unit cell in the crystal consists of an insulin hexamer containing two zinc ions, with two *m*-cresol molecules bound at each dimer−dimer interface stabilizing an R_6 conformation. Six covalently bound lithocholyl groups are arranged symmetrically around the outside of the hexamer. These form specific van der Waals and hydrogen-bonding interactions at the interfaces between neighboring hexamers, possibly representing the kinds of interactions which occur in the soluble aggregates at the site of injection. Comparison with an equivalent nonderivatized native insulin hexamer shows that the addition of the lithocholyl group disrupts neither the important conformational features of the insulin molecule nor its hexamer-forming ability. Indeed, binding studies show that the affinity of *N*-lithocholyl insulin for the human insulin receptor is not significantly diminished.

In a healthy individual, release of insulin from the pancreatic β cells is very sensitively controlled in response to variations in blood glucose levels associated with food consumption during the day and fasting at night. In this way normal blood glucose levels are maintained. For a type I diabetic patient, however, the great majority, if not all, of the insulin-producing cells have been destroyed, and it is therefore necessary to carry out a continuous daily regime of insulin therapy by subcutaneous injection. This is not only inconvenient and sometimes awkward for the patient but also far from ideal, since the erratic diffusion of insulin through the subcutis makes it very difficult to maintain the normal insulin profile. Lack of normoglycemia inevitably leads to long-term complications such as blindness, renal failure and neuropathy, and it is therefore imperative that better methods of insulin therapy be introduced. To this end, recombinant DNA technology and semisynthesis techniques are being used to design novel insulin products with improved pharmacological and therapeutic properties.

Insulin is a 51 amino acid peptide hormone produced in the islets of Langerhans in the pancreas. Its primary function, acting as a monomer, is to facilitate the transport of glucose molecules across the cell membranes of adipose and muscle tissue by binding to and activating a 300 kDa transmembrane receptor. While the exact mode of binding of insulin to its receptor is not known, current understanding is that the insulin molecule is largely enclosed by the receptor, designated surfaces of the hormone being particularly important for receptor binding. A distinctive property of insulin is its ability to associate into hexamers, in which form the hormone is protected from chemical and physical degradation during biosynthesis and storage. X-ray crystallographic studies on insulin show that the hexamer consists of three dimers related by a 3-fold axis of rotation. These dimers are closely associated through the interactions of two zinc ions at its core positioned on the 3-fold axis. The monomeric subunit within each dimer consists of an A and a B chain of 21 and 30 amino acid residues, respectively, which form a compact molecule comprising two α-helices in the A chain and an α-helix and a β-strand in the B chain. The B chain N-terminus is in an extended conformation that is characteristic of the so-called T-state insulin (*1, 2*). Crystallographic studies have also shown that a T_6 hexamer can undergo a conformational transformation to an R_6 hexamer in which the B chain N-termini are α-helical. The R-state is promoted both in the crystal and in solution by the presence of phenol, *m*-cresol, or resorcinol (*2*−*6*).

Zinc and phenolic additives are regularly used in therapeutic insulin preparations to promote hexamer formation as a precaution against degradation during storage. In this

† The coordinates of *N*-lithocholyl insulin have been deposited in the Protein Data Bank at the EBI Macromolecular Structure Database, EMBL Outstation, Hinxton, European Bioinformatics Institute, Wellcome Trust Genome Campus, Hinxton, Cambridge CB10 1SD, United Kingdom, under accession number 1uz9.

* To whom correspondence should be addressed.
‡ University of York.
§ Novo Nordisk A/S.
|| Bioinformatics Institute.

10.1021/bi036163s CCC: $27.50
Published on Web 05/01/2004

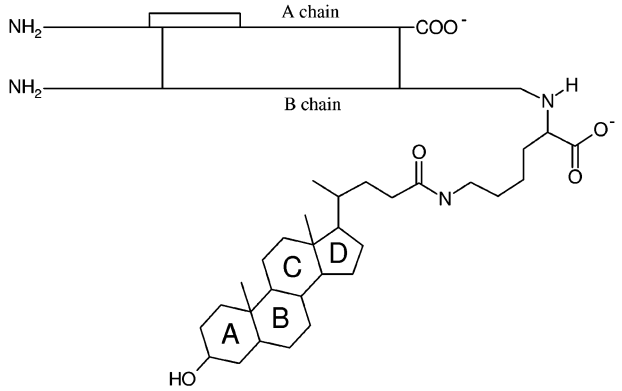

FIGURE 1: Schematic illustration of *N*-lithocholyl insulin showing the peptide bond link between the ϵ-amino group of residue B29 Lys and the lithocholyl group. Residue B30 Thr has been removed in order to locate the negative charge of the C-terminus closer to the lithocholyl group, thereby giving the appearance of a lithocholic acid that enhances the affinity for serum albumin. The hydrocarbon rings of the lithocholyl group are labeled according to standard nomenclature for steroids. This figure was made using ISIS/Draw 2.4 (MDL Information Systems, Inc.).

form, however, the action of injected insulin is delayed while the hexamers diffuse through the subcutis and dissociate into dimers and monomers (*7*). This means that the timing of injections, especially before a meal, has to be judged carefully. A recent innovation in the design of rapid-acting insulins (which cope with the surge of blood glucose associated with a meal) involves the introduction of a hexamer-destabilizing mutation at the monomer−monomer interface of the dimer. This results in faster hexamer dissociation after injection, leading to tighter blood glucose control. Modifications at the B chain C-terminus, including Asp^{B28} and $Lys^{B28}Pro^{B29}$, have been particularly successful and do not detrimentally affect the receptor binding capacity of the molecule (*8*−*11*).

To complement the rapid-acting insulins, attention has now turned to the design of new prolonged-acting insulins that provide improved blood glucose control between mealtimes. Historically, this has been achieved by injecting a slow-dissolving, crystalline suspension of hexameric insulin. In a new approach, the ϵ-amino group of residue Lys^{B29} has been acylated with a long-chain saturated fatty acid (*12*, *13*). This gives the insulin molecule the ability to bind to circulating serum albumin after injection, which slows the activity of the insulin considerably. It has been demonstrated that such new products provide a more even and sustained basal level of insulin than the crystalline products and, being soluble, have none of the complications associated with crystallinity (*14*). Several different acylation groups have been investigated. We here present solution studies and a crystal structure analysis of *N*-lithocholyl insulin, in which residue Lys^{B29} has been acylated with a bile acid derivative (Figure 1).

MATERIALS AND METHODS

Insulin Preparation. Acylated insulin analogues were prepared using conventional peptide chemistry as previously described (*15*). Insulins for size exclusion chromatography (SEC)[1] were prepared as formulations containing 600 nmol of insulin/mL and 2−2.5 Zn^{2+} ions per hexamer, 1.5% glycerol, and 0.3% phenol. Iodination of Tyr^{A14} by $^{125}I_2$ was used to label the compound for binding experiments (*16*).

Table 1: Crystallographic Data Processing and Refinement Statistics

Data Processing Statistics	
$P6_322$ cell dimensions (Å)	$a = b = 51.79$, $c = 68.34$
diffraction limits (Å)	24.00−1.58 (1.61−1.58)[a]
no. of unique reflections	7689
completeness of data	98.0 (98.2)
R_{sym} (%)	3.4 (12.0)
multiplicity	5.9 (5.0)
$I/\sigma I$	33.1 (13.9)
Refinement Statistics	
R_{cryst} (%)	18.0
R-free (%)	20.6
rms Δ bond lengths (1−2) (Å)	0.013 (0.021)[b]
rms Δ angles (deg)	1.821 (2.073)
rms Δ chiral volumes (Å^3)	0.107 (0.200)
mean temperature factors (Å^2)	19.2
Ramachandran (% in most favored area)	97.6

[a] Highest resolution shell statistics given in parentheses. [b] Average geometric restraints given in parentheses.

Crystallization. Crystals of lithocholyl insulin were grown by the sitting-drop vapor diffusion method, using a protocol adapted from the hanging-drop method of Hu et al. (*17*). Initially, tiny hexagonal rod-shaped crystals of lithocholyl insulin were obtained. The crystal size was increased by changing to the sitting-drop method and also by the addition of glucose or detergents to the reservoir solution. Optimum crystallization conditions are as follows: the protein solution consisted of 10 mg/mL lithocholyl insulin in 0.02 M HCl, while the reservoir solution contained 0.5 M Tris-HCl, pH 8.0, 0.1 M trisodium citrate, 2 mM zinc acetate, and 0.05% w/v *m*-cresol. Ten microliters of a 5 mM glucose solution was added to each 1 mL reservoir prior to making the drops, which each consisted of 0.6 μL of protein solution and 1.2 μL of reservoir solution.

Crystallographic Data Collection and Data Processing. A single crystal of dimensions 0.02 × 0.02 × 0.30 mm^3 was vitrified at 120 K in a cryoprotectant solution consisting of 60% (v/v) reservoir solution and 40% (v/v) glycerol, prior to data collection on station 9.6 ($\lambda = 0.87$ Å) at the Daresbury SRS, U.K. A 1.58 Å data set was collected by means of a combination of high- and a low-resolution sweeps, with oscillation angles of 1.0° and 2.0°, respectively. The data were processed using XDISP, DENZO (version 1.9.1), and SCALEPACK (version 1.9.0) from the HKL package (*18*) and SCALEPACK2MTZ, TRUNCATE, and CAD from the CCP4 suite (*19*). Data statistics are shown in Table 1.

Structure Solution and Refinement. The crystal structure of *N*-lithocholyl insulin was solved by molecular replacement as implemented in AMoRe (*20*) using the coordinates for the structure of the NN304 fatty acid acylated insulin (*21*). Cycles of maximum likelihood refinement were then carried out using REFMAC (*22*). Throughout the refinement a randomly selected group of reflections constituting 5% of the total data was excluded for the purpose of *R*-free calculations. This group of data would normally be used for the estimation of σA and the *R*-free calculations. However, in this case the *R*-free data set was found to be too small (353 observations), and therefore σA was estimated using

[1] Abbreviations: HIR, human insulin receptor; HSA, human serum albumin; NN304, Lys^{B29}-tetradecanoyl des-(B30) human insulin; NPH, neutral protamine hagedorn; SEC, size exclusion chromatography.

the working set of data (95% of the total). Periodic manual rebuilding of the protein model and the addition of water molecules to $2F_o - F_c$ and $F_o - F_c$ electron density maps were carried out using XFIT in QUANTA (*23*). The lithocholyl group was first constructed in QUANTA and then modeled into appropriate electron density in the vicinity of residue B29 Lys. Toward the end of the refinement, anisotropic *B*-factors were refined along with atomic positions, yielding a final *R*-factor of 17.78% (*R*-free = 21.17%). Finally, the quality of the geometry of the protein structure was analyzed using PROCHECK (*24*) (Table 1).

Molecular Modeling. To investigate the energies associated with the observed structural deformations in the lithocholyl group relative to deposited crystal structures of lithocholic acid, energy minimizations and conformational interconversion calculations were carried out according to the method in ref *25*.

Aggregation Studies of Insulin Analogues by Size Exclusion Chromatography. Size exclusion chromatography was used to determine the propensity of the insulin analogue to self-assemble. The chromatographic system consisted of a 30 × 1 cm column of Superose 6 HR (Superose 6 HR 10/30, Amersham Pharmacia Biotech). Insulin was eluted at 37 °C with 140 mM NaCl, 3 mM NaN_3, and 10 mM Tris-HCl, pH 7.4, at a flow rate of 0.25 mL/min, and the effluent was monitored by continuous absorbance measurement at 276 nm. The apparent molecular mass was determined using a series of standards following the method of Andrews (*26*). The chromatography procedure was repeated, employing the same buffer system after addition of phenol to a final concentration 8 mM.

Binding Studies. The affinity of acylated insulin analogues for serum albumin was determined as previously described (*13*). Fatty acid free human serum albumin (HSA) was immobilized on divinylsulfone-activated Sepharose 6B MiniLeak (Kem-En-Tec, Copenhagen, Denmark) to a concentration of 0.2 mM suction-dried gel. The immobilized HSA was suspended and diluted to cover the range from 0 to 10 μM in 100 mM Tris-HCl, adjusted to pH 7.4. Triton X-100 (0.025%) was included to prevent nonspecific adhesion. After 2 h of incubation at 23 °C, free and albumin-bound insulin were separated by centrifugation. Plots of bound/free vs albumin concentration were linear, and the apparent association constant K_a was determined from the slope of the plots (*13*).

The affinity of the insulin analogues for the human insulin receptor (HIR) was determined by a microtiter plate antibody capture assay essentially as described in the literature (*27*). Microtiter plates were coated with affinity-purified goat anti-mouse IgG antibody (Pierce, Rockford, IL) in 50 μL/well of 20 μg/mL solution in Tris-buffered saline (TBS): 0.15 M Tris, pH 7.5, and 0.1 M NaCl. The plates were incubated overnight at 4 °C before being blocked with 200 μL of Superblock (Pierce) and then washed twice with binding buffer. Next, a suitable dilution of receptor-specific antibody (F12 made in-house) was added. For this and all subsequent dilutions, 0.1 M Hepes, pH 8.0, was used as a binding buffer. The plates were incubated for 1 h before being washed three times with binding buffer. Then, a suitable dilution of HIR was added, and the plates were incubated overnight at 4 °C before being washed three times with binding buffer. Binding experiments were performed by adding a total volume of 150 μL of binding buffer to 8−10 pM tracer (A14Tyr[^{125}I]-insulin) and varying concentrations of insulin or insulin analogue. After 36 h at 4 °C, unbound ligand was removed by washing three times with cold binding buffer, and the tracer bound in each well was counted with a γ-counter. The binding data were fitted using the nonlinear regression algorithm in the GraphPad Prism 2.01 (GraphPad Software, San Diego, CA).

RESULTS

Crystal Structure. N-Lithocholyl insulin crystallized in space group $P6_322$ (Table 1), giving rise to one molecule of insulin per asymmetric unit. The refined model consists of one molecule of *N*-lithocholyl insulin, one molecule of *m*-cresol, zinc and chloride ions (each 1/3 occupancy), and 57 water molecules. A quality assessment of the structure is given in Table 1. By applying the symmetry operations of space group $P6_322$, the hexamer of *N*-lithocholyl insulin is generated. This trimer of dimers is stabilized by the interactions of two zinc ions symmetrically located 15.7 Å apart on the hexamer 3-fold axis, each one having a tetrahedral coordination sphere consisting of three B10 His side chains (one from each dimer) and a chloride ion (Figure 2). Hexamer stability is enhanced by the interactions of six *m*-cresol molecules buried at the dimer−dimer interfaces. Each one forms two hydrogen bonds between its hydroxyl group and the protein main chain atoms A6 O (2.7 Å) and A11 N (2.9 Å), van der Waals contacts to the side chains of B5 His and B11 Leu through the aromatic ring, and van der Waals contacts to the side chains of A16 Leu and B14 Ala through the methyl group (Figure 3). These interactions were first observed in the crystal structure of native insulin complexed with *m*-cresol (*6*). Additional dimer−dimer contacts include van der Waals interactions between the side chain of residue B2 Val and the main chain atoms of residues A9 and A10 and similar interactions between the zinc-bound chloride ion and the side chain of residue B6 Leu.

Within the monomeric subunit of the hexamer, the conformations of the A and B chains are very similar to those of other insulin molecules. The A chain consists of two α-helices (residues A1−A7 and A12−A20) linked by a short loop (residues A8−A11). The B chain contains a longer section of α-helix (residues B1−B19), followed by a tight loop and then an extended chain region between residues B23 and B29. The close proximity of the two chains is maintained by disulfide bridges joining residues A7−B7 and A20−B19 and a main chain hydrogen bond between A19 O and B25 N. A third disulfide link between residues A6 and A11 forms an intrachain connection. It is interesting that all of the residues involved in these interactions occupy slightly less than ideal positions in a Ramachandran plot. On the whole, the side chains in the insulin molecule are well ordered, with the exception of residues B4 Gln, B9 Ser, B13 Glu (Figure 4), and B17 Leu that occupy two conformations each, and residue A14 Tyr on the outside of the molecule, which is completely disordered. Dimer formation is brought about by β-strand formation between the extended B chain C-termini of two adjacent monomers. Additional monomer−monomer contacts are hydrophobic in nature, involving the side chains of residues A16 Tyr, A21 Glu, B12 Val, B23 Gly, B24 Phe, B25 Phe, B26 Tyr, and B28 Pro.

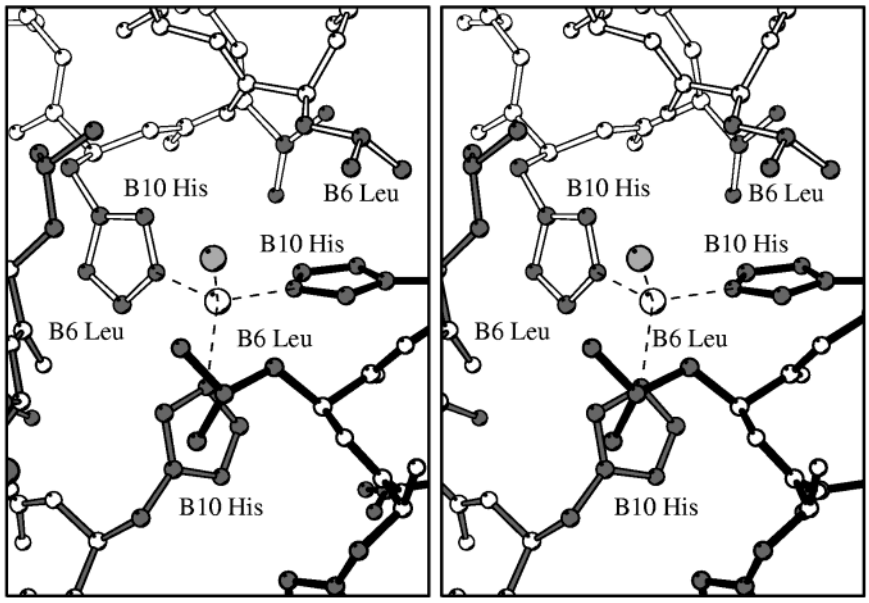

FIGURE 2: Stereoview of one of the zinc ion binding sites at the center of the *N*-lithocholyl insulin hexamer. The zinc ion (large white sphere) is tetrahedrally coordinated to three B10 His side chains and a chloride ion (gray sphere). Each histidine side chain is from a different, symmetry-related dimer, which has either white, gray, or black bonds. All side chain and main chain atoms are colored gray and white, respectively. The coordination distances to the zinc ions (dashed lines) are 2.0 Å for the Nϵ2 atoms of each histidine side chain and 2.2 Å for the chloride ion. This figure was made using BOBSCRIPT (*34*).

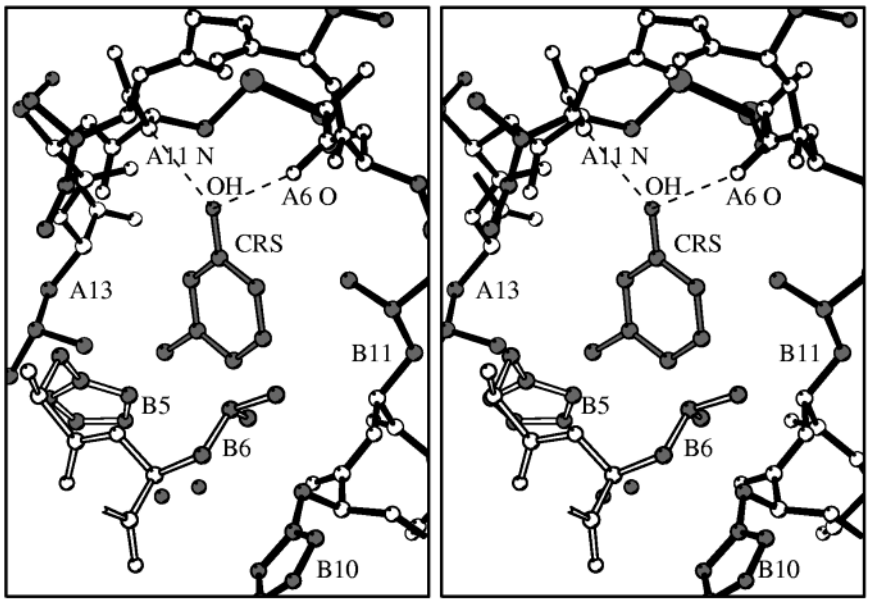

FIGURE 3: Stereoview of one of the *m*-cresol (3-hydroxytoluene, CRS) binding sites at the dimer−dimer interface in the *N*-lithocholyl insulin hexamer. The *m*-cresol interactions include hydrogen bonds between its hydroxy group and the main chain atoms A6 O and A11 N (dashed lines), and van der Waals contacts to various aliphatic side chains including residues A13 Leu, B6 Leu, and B11 Leu of one dimer (black bonds) and B5 His of the adjacent dimer (white bonds). Side chain and main chain atoms are colored gray and white, respectively, and water molecules are shown as gray spheres. This figure was made using BOBSCRIPT (*34*).

Comparison of the *N*-lithocholyl insulin hexamer with other insulin crystal structures shows that its conformation is, as expected, most closely related to that of the R_6 (phenol) insulin hexamer (*4*, *5*). A superposition of insulin monomers from these two hexamers reveals that they are almost identical in conformation, small main chain and side chain displacements in *N*-lithocholyl insulin being confined to the B chain N- and C-termini in the proximity of the lithocholyl group (Figure 5). In particular, the side chain of residue B1 Phe has moved slightly in order to make van der Waals contact with the hydrophobic surface of the lithocholyl group, which otherwise has no contact with the rest of the monomer. This lack of interference between the lithocholyl group and the protein molecule to which it is attached means that neither dimer nor hexamer formation is inhibited by the new group and that, owing to the head-to-tail arrangement of monomers in the dimer, six lithocholyl groups are evenly distributed around the R_6 insulin hexamer (Figure 6).

The lithocholyl group occupies a very stable position at the interface of two hexamers, where it is entirely surrounded by a network of protein atoms and ordered water molecules with which it is able to form compatible interactions. The conformation of this group is quite striking, the A ring being perpendicular to the B, C, and D rings, which are more or

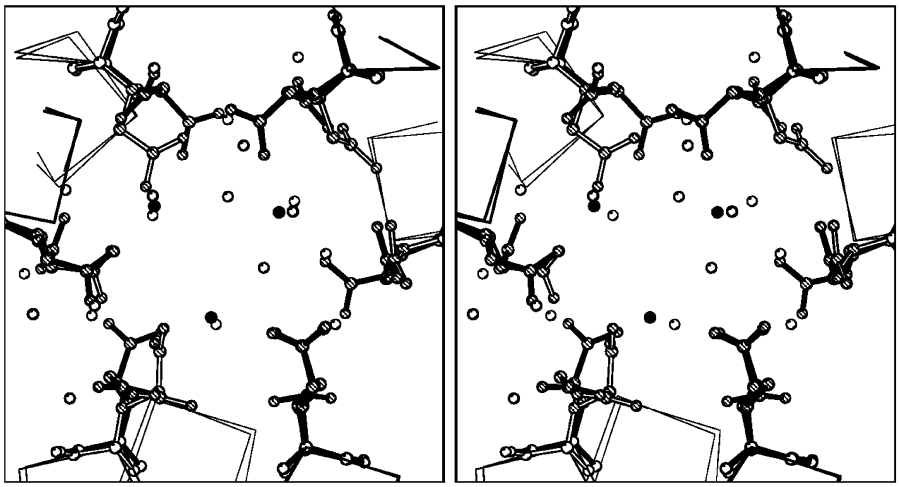

FIGURE 4: Stereoview showing the *N*-lithocholyl insulin hexamer (black bonds and black spheres for water molecules) superimposed on that of the native R6 insulin hexamer (*4*) (white bonds and white spheres for water molecules). In both hexamers, the six B13 Glu residues (ball-and-stick representation, main chain atoms in white, side chain atoms in gray) gather at the center. The conformations of the B13 Glu side chains in the two hexamers are somewhat different, the dual conformation of B13 Glu in the *N*-lithocholyl insulin hexamer displacing some of the water molecules that are present in the native R6 insulin hexamer. This figure was made using BOBSCRIPT (*34*).

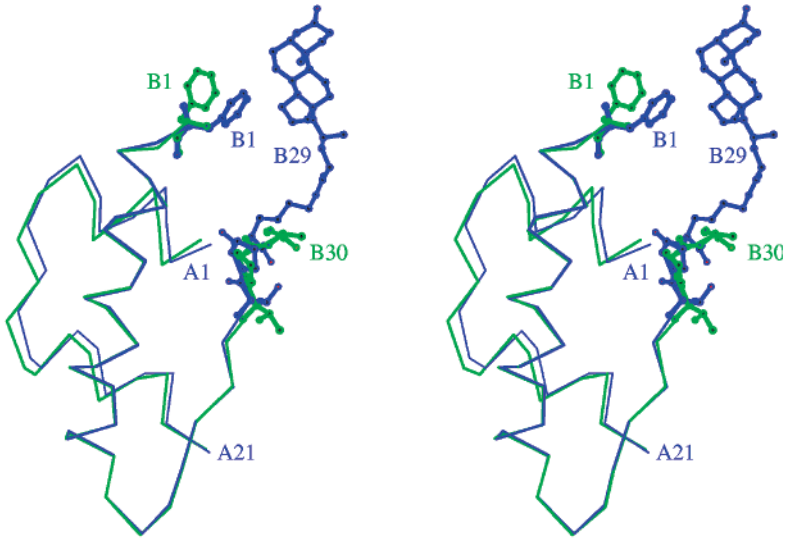

FIGURE 5: Stereoview of one of the six symmetry-related monomers in the *N*-lithocholyl insulin hexamer (in blue) superimposed onto a monomer from the R_6 (phenol) insulin hexamer (in green) (*4*). Residues are represented by their Cα atoms only, except at the B chain N- and C-termini where full atom representation is given to show some minor distortions at residues B1 Phe, B27 Thr, B28 Pro, B29 Lys, and B30 Thr in the proximity of the lithocholyl group. This figure was made using BOBSCRIPT (*34*).

less coplanar (Figures 1 and 7). This enables it to fit into a naturally occurring cleft at the monomer−monomer interface in a dimer of the adjacent hexamer. The end of the lithocholyl group is anchored by two hydrogen bonds from the A-ring carbonyl group to the hydroxyl group of B26 Tyr (Figure 8) and the main chain carbonyl group of B16 Tyr via a water molecule. Other than these, the contacts with the lithocholyl group are entirely hydrophobic in nature, involving residues A3 Val, B1 Phe, B4 Gln, B5 His, B26 Tyr, B28 Pro, and B29 lithochloyl-lysine of one monomer and residues B16 Tyr, B20 Gly, and B21 Glu of the other (Figure 8). In addition, the side chain of residue B1 Phe forms a ring-stacking interaction with a symmetry-equivalent residue, both of which make van der Waals contact with the lithocholyl group. This extensive network of interhexamer interactions, coupled with the solvent-excluding effect of the lithocholyl groups, could explain the observed excellent diffraction characteristics of the lithocholyl insulin crystals.

Molecular Modeling. A comparison of the lithocholyl group in the insulin molecule with crystal structures of lithocholic acid in the Cambridge Structural Database System (CSDS) revealed relatively small deviations in conformation, confined to the A ring and the acidic end of the molecules, although the overall conformations were very similar. Computing the energetics of interconversion between these conformational states yielded 4.0 kcal mol^{-1}, of which 1.5 kcal mol^{-1} originated from changes in the A ring.

Size Exclusion Chromatography. The ability of zinc ion complexes of the analogue to self-assemble was studied by size exclusion chromatography (SEC) (Figure 9). The elution profiles display a single peak in the exclusion volume corresponding to a molecular mass of more than 5000 kDa, followed by a long narrow tail and a small peak in the range 30−6 kDa. Human insulin and NN304 standards displayed a single peak of 20 and 45 kDa, respectively, corresponding to a hexameric or dodecameric assembly. Addition of 2, 4,

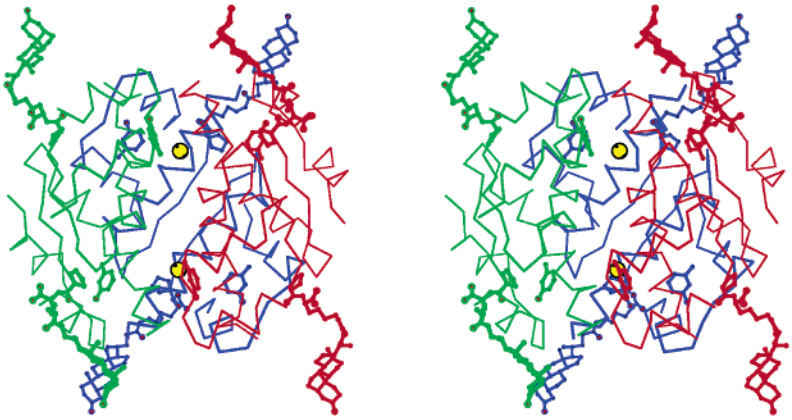

FIGURE 6: Stereoview of the *N*-lithocholyl insulin hexamer. The three dimers are colored red, green, and blue, respectively, and the two zinc ions at the center of the hexamer are shown as yellow spheres. *m*-Cresol (3-hydroxytoluene) molecules, at the dimer−dimer interfaces, and the lithocholyl groups, on the outside of the hexamer, are shown in ball-and-stick representation. This figure was made using BOBSCRIPT (*34*).

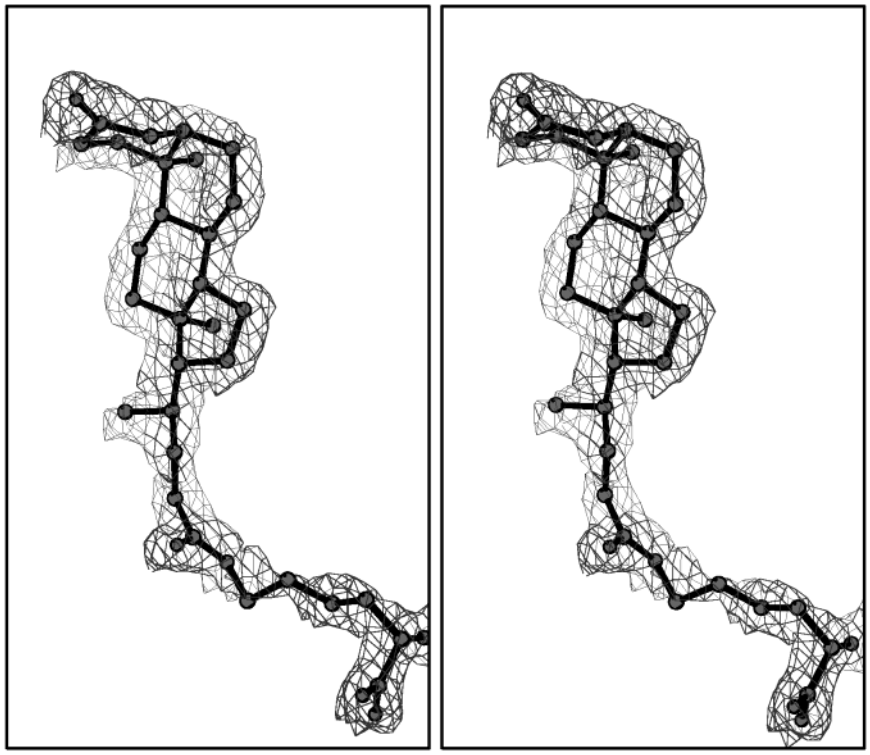

FIGURE 7: Stereoview of the lithocholyl group and residue B29 Lys with associated $2F_o - F_c$ electron density contoured at 1σ. This figure was made using BOBSCRIPT (*34*).

and 8 mM phenol to the eluent resulted in a collapse of the high molecular mass profile to multiple peaks with molecular masses close that of the insulin monomer (Figure 9).

Binding to Serum Albumin and the Insulin Receptor. The binding of the analogue to Sepharose 6B immobilized human serum albumin was measured in a binding assay and compared to that of Lys^{B29}-tetradecanoyl des-(B30) human insulin (NN304), a prolonged-acting insulin containing a C14 fatty acyl group. The *N*-lithocholic acid acylated insulin clearly displays albumin binding properties (Table 2); however, its affinity for human serum albumin is reduced (38%) compared to the acylated insulin standard NN304 (Table 2).

The affinity of the insulin analogue for the human insulin receptor was determined by a microtiter plate antibody capture assay using a receptor-specific antibody, F12. Acylation resulted in a decrease in affinity for the insulin receptor to about 33% compared to human insulin (Table 2). Its affinity is similar to that of the fatty acid acylated insulin, NN304.

DISCUSSION

Current regimes of insulin therapy include the use of two complementary types of insulin: a rapid-acting, monomeric insulin required for the response to the high blood glucose levels associated with a meal, and a prolonged-acting insulin which provides a basal level of the hormone between meals and overnight. For seven decades prolonged action has been achieved by injecting a crystalline suspension of insulin that dissolves slowly at the injection site. This technique is clearly successful, with products such as NPH (neutral protamine hagedorn) and Lente insulins giving action over 13−20 h.

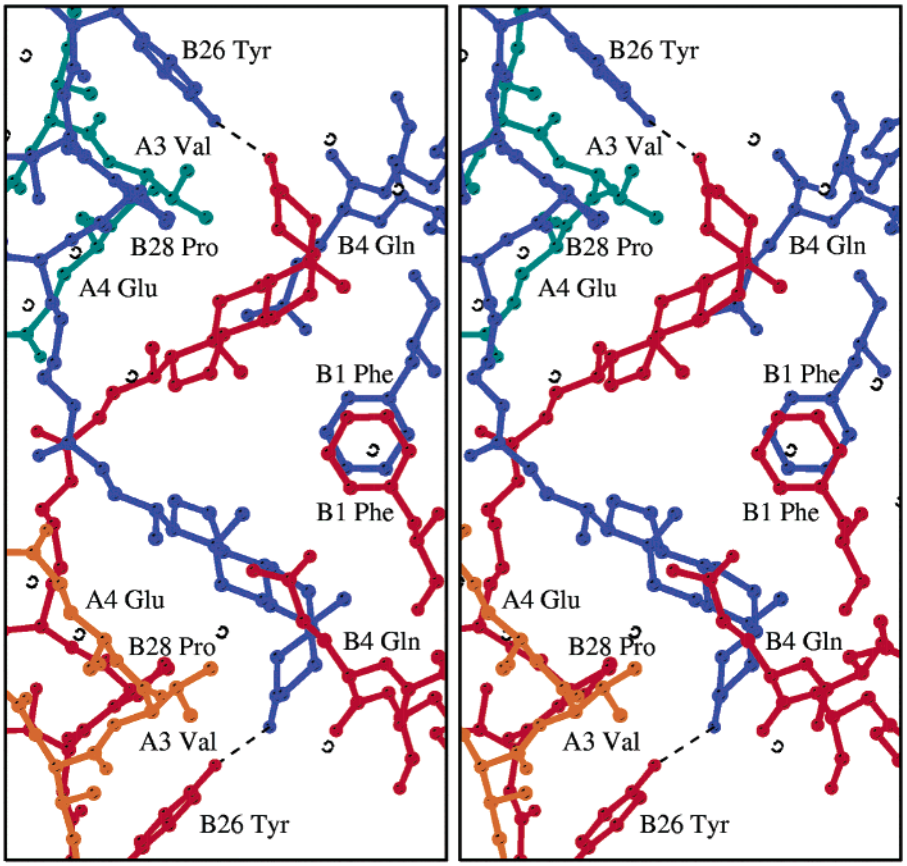

FIGURE 8: Stereoview showing the close proximity of two lithocholyl groups at a hexamer−hexamer interface. Atoms are shown in ball-and-stick representation, with the A and B chains of a monomer from one of the hexamers colored slate blue and blue, respectively, and equivalent residues of the adjacent hexamer colored orange and red, respectively. Many of the side chains in van der Waals contact with the lithocholyl group are shown. An important hydrogen bond, between the A-ring hydroxyl of the lithocholyl group and the hydroxyl group of residue B26 Tyr, is represented by a dashed line. Water molecules are shown as white spheres.

However, these products are associated with some variability of the effect leading to inadequate blood glucose control (*14*). Furthermore, the NPH preparations tend to give a significant peak of insulin activity 4−8 h after injection leading to the possibility of hypoglycemic episodes overnight. A more desirable product would be homogeneous in its makeup and provide a more consistent circulating, low-level concentration of insulin.

Various new approaches to prolonged action are being investigated. A recent innovation involves the covalent attachment of a long-chain fatty acid to the insulin B chain C-terminus (*12*, *13*). This gives the hormone albumin binding properties so that, after injection, insulin action is retarded by reversible binding to this circulating serum protein. The best characterized of these analogues is NN304 [Lys^{B29}-tetradecanoyl des-(B30) insulin] which has a C14 fatty acid attached to the side chain of residue Lys^{B29}. This product is formulated as a solution at neutral pH. In the clinic it provides a prolonged and unique uniform release of insulin after injection (*28*, *29*). In further developments, more sophisticated chemical groups have been attached to the insulin B chain C-terminus. Lithocholic acid is a bile acid derivative whose hydrophobic character gives it a reasonable affinity for serum albumin ($K_a = 2 \times 10^5$ M^{-1}) (*30*). The crystal structure of *N*-lithocholyl insulin reveals that, as with the C14 fatty acid, the addition of a bulky hydrophobic group at the end of the B chain has no significant effect on the conformation of the insulin monomer (Figure 5), nor its ability to form hexamers. Furthermore, a moderate decrease in affinity for the insulin receptor as observed in this study has no impact on the in vivo potency of insulin analogues (*31*) (Table 2). This product is stable, although prolonged storage at low temperature leads to some precipitation.

The appearance of the *N*-lithocholyl insulin hexamer is striking (Figure 6), with the lithocholyl "hooks" transforming a normally hydrophilic, spherical insulin hexamer into a more cylindrical and hydrophobic entity able to aggregate in solution. Interestingly, the size exclusion chromatography studies on lithocholyl insulin suggest that multihexamer aggregates do exist in the absence of phenol but that the addition of phenol to the eluent reduces these aggregates to single hexamers. One explanation for this relates to the T → R conformational transition induced by phenol. In both T_6 and R_6 hexamers, the position of the lithocholyl group would be expected to be the same. However, the environment of the group would change owing to the movement of residue B1 Phe from the dimer−dimer interface to the surface of the hexamer. Thus in the R_6 (phenol-induced) hexamer, residue B1 Phe is in a position to form van der Waals contacts with the lithocholyl group (see Figures 5 and 8). Given the potential flexibility of the lithocholyl/B29 Lys linkage (Figure 1), the interactions with B1 Phe are likely to stabilize the lithocholyl group, thus facilitating lattice contacts and crystallization. If these same interactions exist in solution, they may serve to inhibit the more random interactions between lithocholyl groups of different insulin

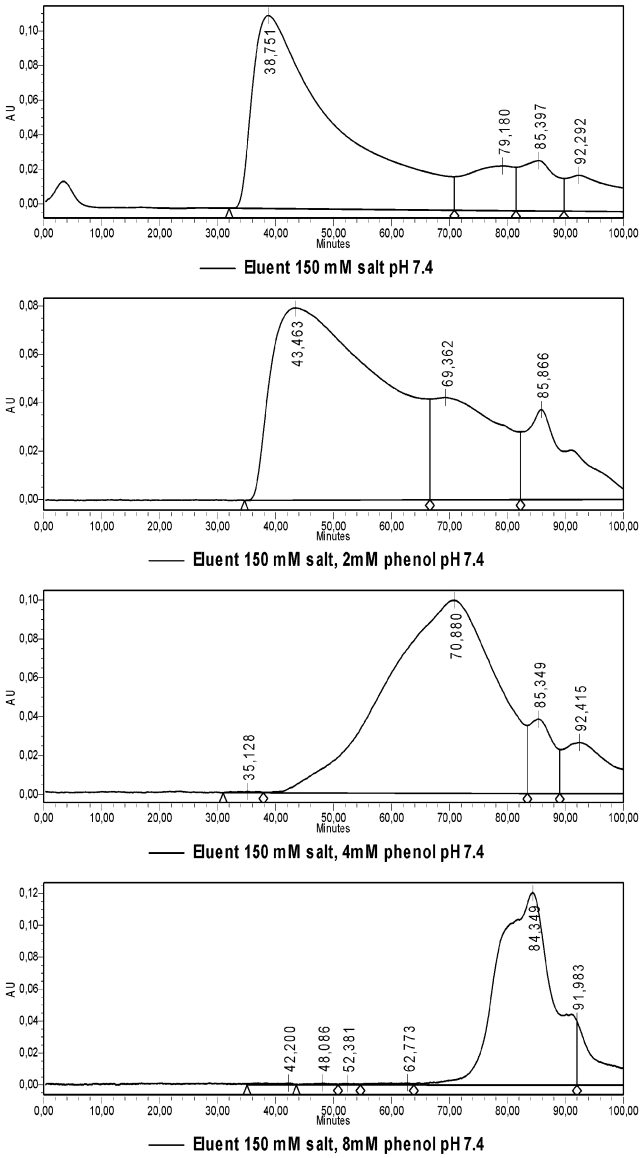

FIGURE 9: Size exclusion chromatography (SEC) profiles of *N*-lithocholyl insulin (absorbance of eluent at 276 nm vs time). The insulin was formulated at neutral pH in the presence of zinc ions and phenol and applied to the column and eluted with 140 mM NaCl, 3 mM NaN_3, and 10 mM Tris-HCl, pH 7.4 at 37 °C. The molecular mass according to SEC was more than 5000 kDa, but the apparent molecular mass decreased to 3 kDa when the column was eluted after addition of phenol, rising to a final concentration of 8 mM.

hexamers which might otherwise lead to aggregation, which happens in the absence of phenol.

In common with the fatty acid chains of NN304 insulin, the crystal contacts made by the lithocholyl group are interhexamer in nature, although the interactions these two groups make in their respective crystal structures are somewhat different. The lithocholyl group is more ordered than the fatty acid chain and makes a greater number of specific hydrophobic and hydrogen-bonding interactions. This is principally a result of its bent conformation, which enables it to fit into a suitably sized niche between the hexamers. The Cambridge Data Base (*32*) contains three lithocholic acid crystal structures, all of which have the same bent conformation as that in the *N*-lithocholyl insulin, although in the latter the atoms of the A ring differ in position by 0.5−0.7 Å. Molecular modeling calculations presented herein suggest that this small structural change, probably necessary to optimize interhexamer hydrogen bonding, has associated with it only a very small energy penalty (approximately 1.5 kcal mol^{-1}). Given the obvious significance of this hydrogen bonding, it is not unreasonable to suppose that it can exist in soluble aggregates in solution as well as in the crystalline state.

Table 2: Binding of Acylated Insulin Analogues to HSA and HIR and Ability of Self-Assembly

	apparent molecular mass (kDa)		binding to	
insulin type	$+Zn^{2+}$ [a]	$+Zn^{2+}$, +phenol[b]	HSA (10^5 L/mol)	HIR (10^9 L/mol)
N-lithocholyl	>5000	3	0.9	1.4
NN304	45	28	2.4	1.2
human	20	25		4.3

[a] The maximum molecular mass observed after size exclusion chromatography analysis of 200 μL of the 0.6 mM insulin analogue formulated in 1.5% w/w glycerol, 30 mM phenol, and two zinc ions per hexamer at 37 °C and the column was eluted by 140 mM NaCl, 3 mM NaN_3, and 10 mM Tris-HCl, pH 7.4, at a flow of 0.25 mL/min. [b] Size exclusion chromatography after addition of phenol to 8 mM to the elution buffer.

Experiments involving subcutaneous injection in pigs of the ^{125}I-labeled analogue in a formulation including zinc and phenol showed a T50% disappearance of more than 34 h, suggesting a more protracted insulin activity of *N*-lithocholyl insulin compared to 14.3 h obtained for NN304 insulin (*33*). The affinity of NN304 for HSA is significantly higher than that of *N*-lithocholyl insulin, and this high affinity is highly correlated with its protracted action (*13*). Although the lithocholyl acylated analogue in this study displays albumin binding properties, it is evident that its main mode of protraction is different from that of NN304 insulin. An additional mechanism has been proposed on the basis of observations from the *N*-lithocholyl insulin crystal structure and the effect of phenol in solution. It is suggested that, after injection of *N*-lithocholyl insulin into the subcutaneous tissue, the phenolic auxiliary compounds rapidly diffuse out of the lithocholyl insulin hexamers, resulting in the formation of a soluble multihexamer complex of the insulin analogue at the site of injection. The slow dissociation of such a structure was found to proceed in a more reproducible manner compared to the dissolution of a crystalline depot (as occurs with NPH). It is likely that the protraction of *N*-litocholyl insulin is governed by this mechanism and albumin binding in an additive manner, ensuring a slow, even release of the insulin into the bloodstream.

ACKNOWLEDGMENT

We acknowledge the use of station 9.6 at the Daresbury SRS for data collection, and we are very grateful to Garib Murshudov and Gerd Schluckebier for useful discussions. We thank the BBRSC for support of the Structural Biology Centre at York.

REFERENCES

1. Baker, E. N., Blundell, T. L., Cutfield, J. F., Cutfield, S. M., Dodson, E. J., Dodson, G. G., Crowfoot Hodgkin, D. M., Hubbard, R. E., Isaacs, N. W., Reynolds, C. D., Sakabe, K., Sakabe, N.,

and Vijayan, N. M. (1988) The structure of 2Zn pig insulin crystals at 1.5 Å resolution, *Philos. Trans. R. Soc. London, Ser. B 319*, 369−456.
2. Kaarsholm, N. C., Ko, H. C., and Dunn, M. F. (1989) Comparison of Solution Structural Flexibility and Zinc-binding Domains for Insulin, Proinsulin and Miniproinsulin, *Biochemistry 28*, 4427−4435.
3. Wollmer, A., Rannefeld, B., Johansen, B. R., Hejnaes, K. R., Balschmidt, P., and Hansen, F. B. (1987) Phenol-Promoted Structural Transformation of Insulin in Solution, *Biol. Chem. Hoppe-Seyler 368*, 903−911.
4. Derewenda, U., Derewenda, Z., Dodson, E. J., Dodson, G. G., Reynolds, C. D., Smith, G. D., Sparks, C., and Swenson, D. (1989) Phenol stabilizes more helix in a new symmetrical zinc insulin hexamer, *Nature 338*, 594−596.
5. Smith, G. D., and Dodson, G. G. (1992) The structure of a rhombohedral R_6 insulin hexamer that binds phenol, *Biopolymers 32*, 441−445.
6. Smith, G. D., Ciszak, E., Magrum, L. A., Pangborn, W. A., and Blessing, R. H. (2000) R-6 hexameric insulin complexed with *m*-cresol or resorcinol, *Acta Crystallogr. D56*, 1541−1548.
7. Brange, J. (1987) *Galenics of Insulin*, Springer, Berlin.
8. Brange, J., Ribel, U., Hansen, J. F., Dodson, G., Hansen, M. T., Havelund, S., Melberg, S. G., Norris, F., Norris, K., Snel, L., Sørensen, A. R., and Voigt, H. O. (1988) Monomeric insulins obtained by protein engineering and their medical implications, *Nature 333*, 679−682.
9. Brems, D. N., Alter, L. A., Beckage, M. J., Chance, R. E., DiMarchi, R. D., Kenney Green, L., Long, H. B., Pekar, A. H., Shields, J. E., and Frank, B. H. (1992) Altering the association properties of insulin by amino acid replacement, *Protein Eng. 5*, 527−533.
10. Ciszak, E., Beals, J. M., Frank, B. H., Baker, J. C., Carter, N. D., and Smith, G. D. (1995) Role of C-terminal B-chain residues in insulin assembly: the structure of hexameric $Lys^{B28}Pro^{B29}$-human insulin, *Structure 3*, 615−622.
11. Whittingham, J. L., Edwards, D. J., Antson, A. A., Clarkson, J. M., and Dodson, G. G. (1998) Interactions of Phenol and *m*-Cresol in the Insulin Hexamer, and Their Effect on the Association Properties of B28 Pro → Asp Insulin Analogues, *Biochemistry 37*, 11516−11523.
12. Kurtzhals, P., Havelund, S., Jonassen, I., Kiehr, B., Larsen, U. D., Ribel, U., and Markussen, J. (1995) Albumin binding of insulins acylated with fatty acids: Characterization of the ligand-protein interaction and correlation between binding affinity and timing of the insulin effect in vivo, *Biochem. J. 312*, 725−731.
13. Markussen, J., Havelund, S., Kurtzhals, P., Andersen, A. S., Halstrøm, J., Hasselager, E., Larsen, U. D., Ribel, U., Schäffer, L., Vad, K., and Jonassen, I. (1996) Soluble, fatty acid acylated insulins bind to albumin and show protracted action in pigs, *Diabetologia 39*, 281−288.
14. Guthrie, R. (2001) Is There a Need for a Better Basal Insulin?, *Clin. Diabetes 19*, 66−70.
15. Saunders, D. (1974) Some Semisynthetic Studies on Insulin, Ph.D. Dissertation, University of Cambridge, U.K.
16. Jorgensen, K. H., and Larsen, U. D. (1980) Homogeneous mono-^{125}I-insulins. Preparation and characterisation of mono-^{125}I-(tyr A14) and mono-^{125}I-(tyr A19)-insulin, *Diabetologia 19*, 546−554.
17. Hu, Y.-L., Wu, B.-M., Zhang, Y., Wang, D.-C., Kaarsholm, N. C., and Norris, R. (1992) *Chin. Sci. Bull. 37*, 1390−1393.
18. Otwinowski, Z., and Minor, V. (1997) Processing of X-ray Diffraction Data Collected in Oscillation Mode, *Methods Enzymol. 276*, 307−326.
19. Collaborative Computational Project, Number 4 (1994) The CCP4 Suite: Programs for Protein Crystallography, *Acta Crystallogr. D50*, 760−763.
20. Navaza, J. (1994) An automated package for molecular replacement, *Acta Crystallogr. A50*, 157−163.
21. Whittingham, J. L., Havelund, S., and Jonassen, I. (1997) Crystal Structure of a Prolonged-acting Insulin with Albumin-Binding Properties, *Biochemistry 36*, 2826−2831.
22. Murshudov, G. N., Dodson, E. J., and Vagin, A. A. (1997) Refinement of macromolecular structures by the maximum-likelihood method, *Acta Crystallogr. D53*, 240−255.
23. Oldfield, T. J. (2001) A number of real-space torsion-angle refinement techniques for proteins, nucleic acids, ligands and solvent, *Acta Crystallogr. D57*, 82−94.
24. Laskowski, R. A., MacArthur, M. W., Moss, D. S., and Thornton, J. M. (1993) PROCHECK: a program to check the stereochemical quality of protein structures, *J. Appl. Crystallogr. 26*, 283−291.
25. Tang L., Whittingham, J. L., Verma, C. S., Caves, L. S., and Dodson, G. G. (1999) Structural Consequences of the B5 Histidine → Tyrosine Mutation in Human Insulin Characterized by X-ray Crystallography and Conformational Analysis, *Biochemistry 38*, 12041−12051.
26. Andrews, P. (1970) Estimation of molecular size and molecular weights of biological compounds by gel filtration, *Methods Biochem. Anal. 18*, 1−53.
27. Mynarcik, D. C., Williams, P. F., Schaffer, L., Yu, G. Q., and Whittaker, J. (1997) Identification of common ligand-binding determinants of the insulin and insulin-like-growth-factor-1 receptors—insights into mechanisms of ligand-binding, *J. Biol. Chem. 272*, 18650−18655.
28. Vague, P., Selam, J. L., Skeie, S., De, L. I., Elte, J. W., Haahr, H., Kristensen, A., and Draeger, E. (2003) Insulin detemir is associated with more predictable glycemic control and reduced risk of hypoglycemia than NPH insulin in patients with type 1 diabetes on a basal-bolus regimen with premeal insulin aspart, *Diabetes Care 26*, 590−596.
29. Hermansen, K., Madsbad, S., Perrild, H., Kristensen, A., and Axelsen, (2001) Comparison of the soluble basal insulin analogue insulin detemir with NPH insulin: a randomized open crossover trial in type 1 diabetic subjects on basal-bolus therapy, *Diabetes Care 24*, 296−301.
30. Roda, A., Cappelleri, G., and Aldini, R. (1982) Quantitative aspects of the interaction of bile acids with human serum albumin, *J. Lipid Res. 23*, 490−495.
31. Ribel, U., Hougaard, P., Drejer, K., and Sorensen, A. R. (1990) Equivalent in vivo biological activity of insulin analogues and human insulin despite different *in vitro* potencies, *Diabetes 39*, 1033−1039.
32. Berman, H. M., Westbrook, J., Feng, Z., Gilliland, G., Bhat, T. N., Weissig, H., Shindyalov, I. N., and Bourne, P. E. (2000) The Protein Data Bank, *Nucleic Acids Res. 28*, 235−242.
33. Havelund, S., Balschmidt, P., Jonassen, I., and Hoeg-Jensen, T. (2002) Aggregates of human insulin derivatives, Novo Nordisk A/S. PCT/DK98/00461(WO 99/21888).
34. Esnouf, R. M. (1997) An extensively modified version of MolScript that includes greatly enhanced colour capabilities, *J. Mol. Graphics 15*, 132−134.

BI036163S